

SAMPLING NEARSHORE FLOWS WITH WAVE-AVERAGED MOVIES

Rob Holman¹, David Honegger² and Merrick Haller³

Abstract

The dominant signal in nearshore images is that of ocean waves. However, when images are averaged over at least several wave periods, a number of residual signatures are revealed that can be exploited to reveal nearshore flow, ocean fronts, or dynamic features in estuaries. These features can be caused by wave breaking at large and short wave scales, variation in wave steepness, and variations in water column turbidity. These in turn can be driven by, hence signatures of, a number of oceanographic phenomena like surface current convergences and estuarine or ocean fronts. Because light and radar waves interact with the ocean surface differently, they are sensitive to different features. Radar is good at seeing frontal features and convergences, for example due to rip currents, while the strongest optical signals result from surface foam and water turbidity. While both X-band radar and optical cameras receive strong signals from surf zone breaking, optics is better able to resolve the short scales of foam patches that help visualize nearshore circulation.

Key words: Argus, marine radar, optics, surf zone circulation, estuaries, remote sensing

1. Introduction

Our understanding of the nearshore has always been limited by our ability to make actual measurements in this complex and often hostile domain. Traditionally these were done using a variety of in situ methods including pressure sensors, current meters and various surveying methods. But costs and logistical difficulties meant that measurements were infrequent and usually geographically limited to some research site or special project.

The discipline of nearshore remote sensing (NRS) has slowly grown as an alternative that allows low-cost measurement over large areas and extensive periods of time, but often with less accuracy than traditional sensors. While the bulk of the development has been based on optical systems (cameras and video), there has been substantial progress in the use of radar, infrared sensors and Lidar. The goal of this work has been to develop alternate NRS methods for measuring all of the needed variables using only remote sensing methods.

There have been a number of successes. The use of temporal averaging, or “time exposure” methods to visualize wave dissipation patterns (Lippmann and Holman 1989) provided a simple method to see and measure nearshore sand bar morphology, rip channels, and shoreline location on an hourly basis for years. Information at shorter time scales can be extracted through pixel time series methods to measure hydrodynamic variables including wave runoff (Holman and Guza 1984), wavenumber, bathymetry derived from wave celerity observations (Stockdon and Holman, 2000; Holman, Plant et al. 2013), wave roller lengths (Haller and Catalan, 2009), wave transformation and setup, (Flores et al, 2016) and the longshore component of surf zone currents (Chickadel, Holman et al. 2003).

These methods have also been applied to marine radar time series for similar applications, such as sand bar morphology (e.g. Ruessink et al., 2002), bathymetry (e.g. Bell 2011), rip current occurrence (Haller et al., 2014), wave transformation (Díaz Méndez et al., 2015), and likewise to thermal infrared sensors for wave dissipation (Jessup et al., 1997; Carini et al., 2015). In some applications, co-located information from multiple sensor time series can be utilized, for example for wave roller measurements (Haller &

¹College of Earth, Ocean and Atmospheric Sciences, 104 Ocean Admin Bldg, Oregon State University, Corvallis, Oregon USA, 97330, holman@coas.oregonstate.edu

²Civil and Construction Engineering, College of Engineering, Oregon State University, Corvallis, Oregon, USA, 97330. honegger@oregonstate.edu.

³Civil and Construction Engineering, College of Engineering, Oregon State University, Corvallis, Oregon, USA, 97330. Merrick.Haller@oregonstate.edu.

Lyzenga, 2003; Catalan et al., 2011), bathymetry and nearshore currents (van Dongeren et al., 2008; Wilson et al., 2014). A good summary of the status of nearshore remote sensing is given by Holman and Haller (2012).

While progress has been good, there are still important areas of weakness. Most notable is the poor ability to measure wave heights. In addition, with some exceptions we are still weak in our ability to measure nearshore circulation, a very important aspect of nearshore geomorphological response. This latter issue is the focus of the current paper (pun intended).

The primary issue is one of isolating signals of currents from the much strong signatures of ocean waves. The success in estimating the longshore component of currents (Chickadel, Holman et al. 2003) depends on the fact that the two signals are mostly orthogonal – waves largely propagate in the cross-shore direction so that both the sampling array and the analysis can be optimized for the detection of longshore currents and the reduction of cross-shore signals. However, for the cross-shore component of flow, the optical signatures of flows are usually small compared to those of wave orbital motions and hence difficult to extract.

The goal of this paper is to investigate new (and rather simple) methods to remove the noise from wave orbital signals to yield good signals from nearshore circulation. This will be done by wave averaging. In the following we will start with a discussion of the long-accepted time exposure method of wave averaging to reveal morphology before extending to shorter averaging time scales that reduce wave signatures but retain those of some surprising tracer signals that appear once the waves are removed. We will discuss the physics by which several sensors image the ocean surface as a key to understanding wave-averaged results, then we will show several examples in terms of the visualization capability before discussing methods of and problems in quantification. This is ongoing research, so some aspects still need solution.

2. Wave Averaging

2.1. Time Exposure Images

Wave averaging has been used for decades in time exposure (timex) images to smooth through the incident waves and leave only the geographical pattern of underlying sand bar morphology. Figure 1 shows an example snapshot-timex image pair from Palm Beach, Australia, collected on Feb. 27, 1996. For such a simple technique, the new visualization capability was remarkable, revealing a complex offshore sand bar with incised rip channels, clear signatures of the shoreline and even short scale transverse bars that were unexpected and even hard to measure once seen (Konicki and Holman 2000).



Figure 1. Example snapshot-time exposure pair from Palm Beach, Australia from Feb 27, 1996.

The goal of time exposures is to remove all signatures of individual waves, leaving only average dissipation patterns that exist because of underlying bathymetry anomalies (sand bars). To average over not just individual waves but also over wave groups, a long averaging period of ten minutes is chosen. Presumably shorter dwell would be sufficient for short wave domains like large lakes and seas, and longer might be appropriate for long Pacific Ocean waves, but ten minutes are used in all cases for simplicity.

2.2. Wave-averaged Images

If our goal is to simply average out waves without concern for wave groups, shorter averaging times can be used with the sequence of consecutive averaged images providing a visualization of water movement. This was originally tried for optical data by Suanda et al (2014) who found out rather fortuitously that one minute averages removed wave clutter but left behind weaker signal like slicks and turbidity variability that could be used to track water movement or internal waves (Figure 2). The residual signatures (often slicks) were not present in all images but depended on wind conditions (surfactants that make the slicks break up under higher winds).



Figure 2. Example one-minute wave-averaged image from Agate Beach, Oregon. Slicks are revealed once the clutter of ocean waves are removed. By display these images in sequence (every minute), the movement of these features is revealed.

Using X-band marine radar, wave-averaged frames were also used to yield impressive visualizations of the wander of rip currents at an open beach environment (Duck, NC) by Haller et al. The method was also applied using X-Band marine radar by Honegger et al (2016) to analyze internal hydraulic jumps in a large estuary, the Columbia River mouth. Using one-minute averaging, they were able to easily visualize the movement of these current fronts with the changing tide and relate surface signatures to the underlying stratification. Similar features are seen in optical wave-averaged images. Also contained in those observations are signals from the incoming salt wedge on flood tides, which can be seen in wave-averaged images from both radar and optical cameras. For example, Figure 3 shows a comparison of synchronous single wave-averaged frames from radar and optical (Argus).

One minute averaging was also applied for optical signals on several ocean beaches. However, results were mostly disappointing with no obvious circulation revealed in the surf zone although the movement of

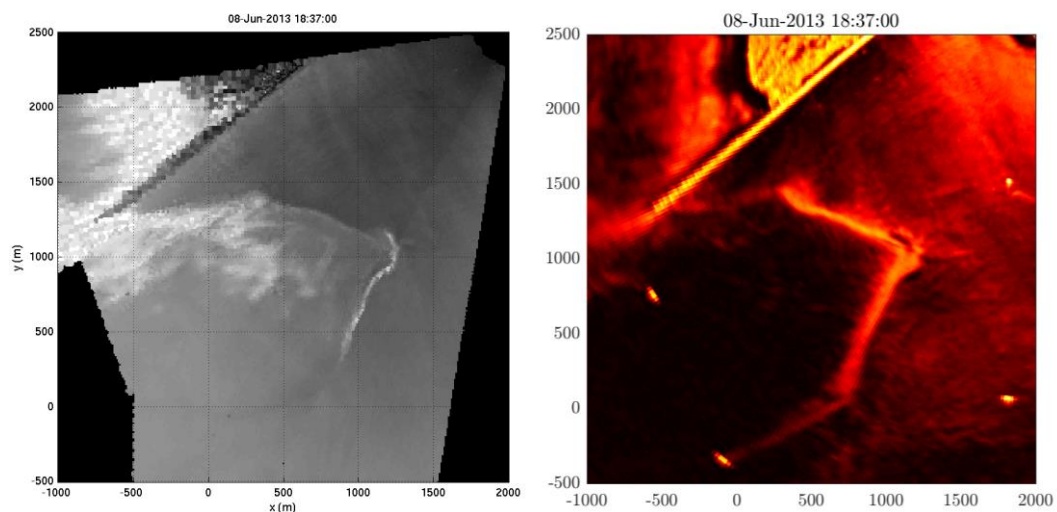


Figure 3. Example one-minute time exposure image taken by radar (left) and the corresponding frame from an optical (Argus) system (right). Each system has different imaging physics so sees some different and some similar features.

offshore water mass fronts was made more obvious. However, recent tests with averaging times reduced to as little as 20 seconds have yielded clear evidence of cell circulation at Duck, NC, through the advection of ephemeral bubble clouds. These empirical results suggest a deeper consideration of the available signals and imaging methods.

3. Signature Physics in Wave-averaged images

The following discussion compares the image physics for three common sensors, marine radar, thermal infrared, and optical cameras. While infrared has not been part of this study, inclusion of infrared sensitivities in our discussions is useful.

3.1 Imaging Physics

X-band marine radar, optical sensors and IR sensors all use electromagnetic radiation that interacts with the dielectric surface of the ocean in ways that depend on their electromagnetic wavelength. X-band radar has the longest wavelength at roughly 3 cm. There is essentially no penetration into the water and backscatter comes in the form of Bragg reflection or re-radiation from surface discontinuities. Thus radar is sensitive to short capillary waves or water “edges” such as in a breaking wave or in surface bubble clouds. Basically radar sees short-scale roughness. As a consequence, radar can see fronts clearly where short wave properties often change rapidly due to current convergences at the front. Similarly they can see the heads of rip currents where incoming wind chop over-steepens as they encounter the adverse currents. In the absence of short wind waves, marine radar signals become small, so wind is important to radar imaging.

Electromagnetic waves in the thermal infrared band are much shorter, with a wavelength of order 10 microns. They also barely penetrate the top millimeter of the ocean so primarily sample the ocean surface. The imaging physics can be complicated. In contrast to the other sensors, infrared is sensitive to temperature and the ocean acts as a black body radiator of IR energy with a strong sensitivity to the angle of observation relative to the surface normal. There is often a thin (millimeter) cool surface layer due to evaporation that, when disturbed by turbulence or wind, can yield visible coherent structures that can be used as passive tracers. Foam from breaking waves appears warm initially but visibly “cools” (reducing radiation) in seconds. There is also substantial IR radiation that comes from the skydome and clouds that partially reflects from the ocean surface. Typically infrared images are rich in features but complex in imaging physics.

Optical signals are the shortest with wavelengths in a narrow band of 0.4-0.7 microns (i.e. humans can see only a small fraction of ambient electromagnetic radiation in which we are immersed). Unlike the other bands, there can be substantial penetration of the water column depending on water clarity, and even reflection off the bottom (variations in the attenuation of different light colors as they reflect from the bottom and are imaged in overhead cameras are used to estimate depth). For most mid-latitude coastal waters there is enough suspended material in the water column to attenuate incident light within meters of the water surface so that cameras see only light backscattered from the water column and light reflected from the surface. Optical radiation that scatters off material in the water back through the surface where it can be seen by a camera is termed “upwelled” radiation and is the dominant signal for near-nadir imaging (looking nearly straight down). However as viewing angles rise toward the horizon, upwelled radiation becomes small compared to light that reflects from the skydome off the ocean surface. Light is also especially well scattered by breaking waves and foam, but in contrast to radar or IR, the strong backscatter from foam is due to the cumulative of partial reflections from the many bubble surfaces in the foam. As with radar and IR, reflection from bubble clouds is omni-directional (termed Lambertian scattering in optics).

3.2 The Results of Averaging

The above knowledge helps us understand the nature of wave-averaged image signals. Because of the water penetration of optical data, these images are sensitive to variability in water column turbidity, something that has no signature in radar or IR (although turbidity may be indirectly visible in IR due to greater water column warming as sunlight is captured by upper water column turbidity). On the other hand, radar is sensitive to changing surface roughness, for example due to short wave convergence and

over-steepening that might not have any optical signature. Both sensors are strongly sensitive to wave breaking (for different reasons). Radar is mostly sensitive to the increased roughness whereas optics sees strong backscatter from bubble clouds and foam and even submerged bubble as they rise to the surface. Breaking events are the strongest signal for all three sensors.

The desired amount of wave averaging depends on the time scales of the signatures that will be exploited. Since the original time exposure method was designed for imaging morphological features, we simply average over ten minutes since that is long compared to other scales or variability like wave groups and the associated intermittent breaking but short compared to morphological time scales. For imaging currents, we need to see features with qualities of passive tracers, i.e. signatures that flow with the water and are visible for sufficiently long to see measurable drift. One minute would seem like a good choice for turbidity features or those associated with tidal fronts. However, if we wish to exploit foam from breaking waves, one minute is too long. A bubble cloud from a breaking front is certainly a strong signature, but visual observations show that these events disappear on the time scale of several wave periods. Thus 20 seconds seems more appropriate for visualizing nearshore circulation based on the advection of foam.

4. Representative Example Images

While the presentation of movies and visualization concepts is not suited to a fixed-text paper like this, we can choose some example images to illustrate the various mechanisms in imaging with different sensors (recognizing that the conference presentation will allow complete visualization). The image pair in Figure 3 illustrates some of the larger-scale features of wave-averaging from the mouth of the Columbia River. The imaged area is 3 by 3 km, with moderately coarse resolution and shows the tidal front from the incoming flood tide as it was proceeding from west (left) to east (right). The oblique linear feature near the top of each frame is the north jetty. In this case, the imaged features are large and easily persistent on minute-to-minute time scales, so one or two minute averaging is appropriate. Both optical and radar clearly see the tidal front as a strong reflector although it is stronger and broader in the radar due to short wave steepening and breaking that is apparent in the optical snapshots but shows greater contrast in radar. On the other hand, optical data captures a great deal of residual foam behind the front that does not have enough roughness at radar length scales and so appears dark. In addition, the radar image of the nose of the advancing front shows two light features extending to the right at slightly different angles. This is not visible in the optical image and its source is unknown.

While the residual foam is an obvious optical feature, the visible band is also able to pick up more subtle color or brightness variations due to differences in water column turbidity. Figure 4a shows a panoramic merge (joining four adjacent oblique images) snapshot from 00:59:59 GMT, June 27, 2013. The image was chosen because several different water masses are evident associated with the tidal front. The front on the right has an associated residual foam streak, indicating a surface flow convergence and accumulated foam. The boundary on the middle and left is more subtle and associated with turbidity differences. It was expected that these boundaries would not be apparent on radar due to the lack of associated roughness, but Figure 4b does show corresponding features. We continue to investigate.



Figure 4a. Oblique panorama of snapshots from the Argus Station at the Columbia River, looking west. The north jetty is visible on the right side of the image. Three water masses are distinguishable due to their different turbidity. The smudge on the top left is a rain drop on the camera lens.

Imaging flow and circulation in the surf zone is more difficult. Figure 5 shows a single gray-shade frame from a quadcopter video taken as Duck, NC in 2015 that has been wave averaged over 30 seconds. Offshore there is a clear water mass boundary that moves from minute to minute and could easily be resolved in one or two-minute averages. However, the breaking patterns in the surf zone also show residual patchiness and structure whose movement is obvious in movies (movie frames usually computed every 15 seconds). Since the lifetime of identifiable features in foam patches is often less than one minute, averaging for a full minute will remove much of this signal and circulation is not visually apparent. In fact, 20-second average appears to be adequate to remove the clutter from individual waves while retaining the foam patchiness whose advection is quite apparent. In this case, there is clear gyre to the north of the pier as well as a clear rip current just on the south side of the pier. In general, short averaging seems to be preferred for surf zone circulation where the primary features for tracking are breaking waves and foam.

5. Complications and Future Work

To advance science we must be able to measure the flows, not just visualize them. This requires that the observed features act as passive tracers, i.e. they advect with the speed of the surrounding flows. The most common method of estimating currents then is Particle Image Velocimetry, or PIV, which assumes that the imaged features are equivalent to particles whose velocity between time samples can be derived from its movement, found by some kind of lag correlation method or equivalent. The extension from point particles to blob-like features works as long as the shape of the feature is unchanging and the analysis averages over the scale of the features.

As an alternate to PIV analysis, Chickadel et al (2003) developed a spectral method for one horizontal dimension (the longshore dimension for measuring longshore currents) in which the slope of the dominant energy in frequency-wavenumber space (after 2D Fourier transform) is used to estimate the velocity. This approach has the advantage of being robust to the wavelength content of the

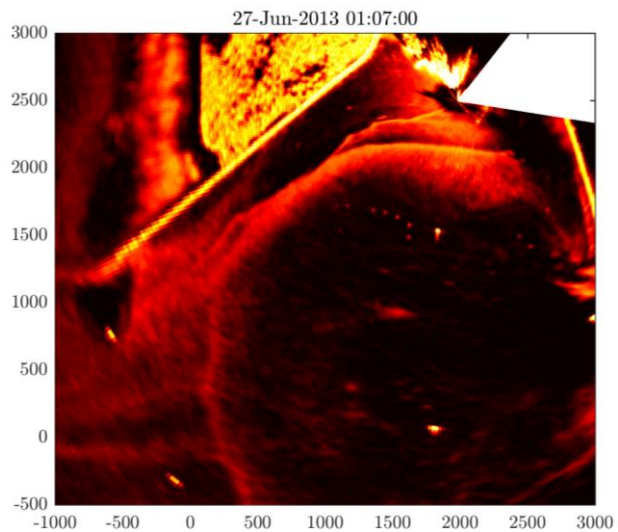


Figure 4b. Equivalent wave-averaged radar image from 0107 GMT, 06/27/17. Water mass boundaries are also imaged in radar, despite having no visible roughness signatures.

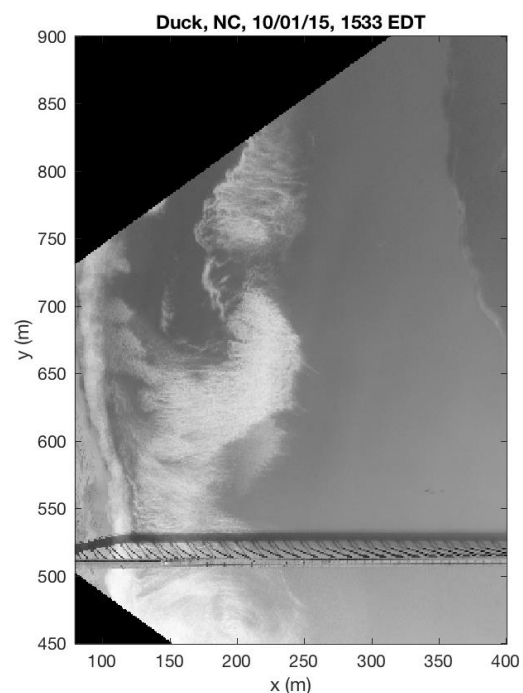


Figure 5. Example 30 s wave-averaged from Duck, NC, collected by a quadcopter. The horizontal line is the Duck pier. An ocean front is visible offshore. Within the surf zone there many features remain even after averaging have removed the wave signatures. Sequences of frames show a gyre to the north of the pier and a rip current just south of the pier.

sample, but has the disadvantage of producing only one component of the two-dimensional flow. Also, like PIV methods, the observed features must be passive tracers.

The analysis of surf zone flows such as are represented in Figure 5 would likely be successful using either method. However, Figure 6 shows an example one-minute wave-averaged frame from the Columbia River that would not be so successful. The strongest contrast features in this image are two wave groups. The first has short waves that appear to be radiating from the top right of the figure, a headland on which the cameras and radar are mounted. These are internal waves that are clearly propagating, in this case at speeds of less than 1 m/s. The second wave group features are larger, just south of the north jetty. From the sequence of movie frames these appear to be moving slowly toward the camera (to the east northeast), in the opposite direction of the first set of internal waves (at other times the features even diverged, indicating a dynamics that we have yet to understand). These also appear to be surface signatures from some dynamics to do with the salt wedge stratification, but these structures do not appear to be propagating with the same speed as weaker turbidity features (i.e. the water).

Methods for partitioning the signals from passive tracers and dynamic features are currently under study.

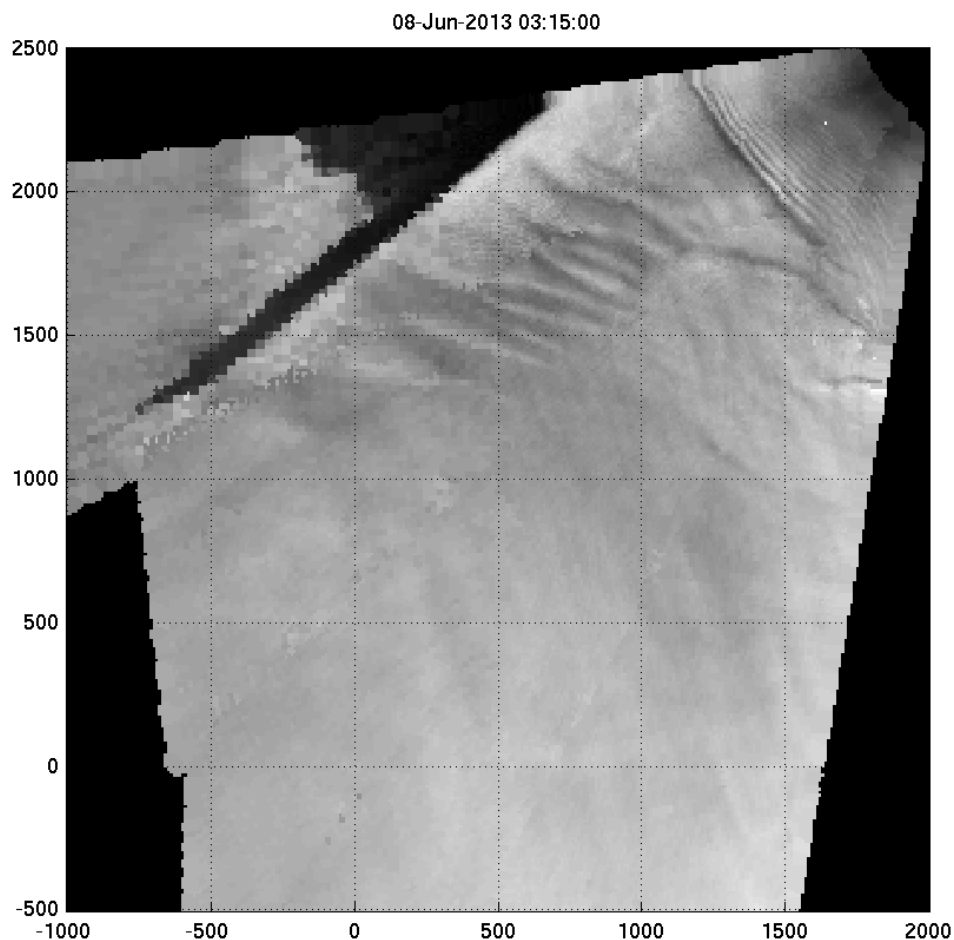


Figure 6. Example one-minute wave-averaged optical frame of the mouth of the Columbia River, with the jetty near the top of the image. Two sets of internal waves are seen, both with apparently different dynamics. Internal waves are progressive so confuse methods used to estimate flow by pattern movement.

6. Summary

When nearshore images are averaged over at least incident wave time scales, the residual images often reveal surprising signatures due to wave breaking, variable turbidity or oceanographic features like tidal or water mass fronts. The nature of these residual, or wave-averaged, images depends on the sensor. Radar signals are dominated by short-scale roughness, and so fronts or rip currents are observable due to the impact of current convergences on short wave steepening or breaking, but radar does not directly see into the water column. By contrast, optical images sense into the water column so can see changes in water mass or turbidity as well as surface signatures. Both sensors strongly see wave breaking, although by different imaging mechanisms.

Quantification of observed flows depends on an assumption that features are passive tracers. This works well in unstratified domains like the surf zone but can be problematic in estuarine domains where various types of internal wave dynamics yield progressive features. Separation of progressive and passive features is an active research topic.

Acknowledgements

Wave averaging work has developed over many years and is not easily linked to any single grant. We thank the Office of Naval Research, the U.S. Army Corps of Engineers, and the USGS for their ongoing support. As always, we thank John Stanley for making things work.

References

- Bell, P. S. and J. C. Osler (2011). "Mapping bathymetry using X band marine radar data recorded from a moving vessel." *Ocean Dynamics* 61: 2141-2156.
- Carini, R. J., C. C. Chickadel, A. T. Jessup and J. Thomson (2015). "Estimating wave energy dissipation in the surf zone using thermal infrared imagery." *Journal of Geophysical Research* 120(6): 3937-3957.
- Catalan, P. A. and M. C. Haller (2008). "Remote sensing of breaking wave phase speeds with application to non-linear depth inversions." *Coastal Engineering* 55(1): 93-111.
- Catalan, P., M. Haller, R. A. Holman and W. J. Plant (2011). "Optical and microwave detection of wave breaking in the surf zone." *IEEE Transactions on Geosciences and Remote Sensing* 49(6): 1879-1893.
- Chickadel, C. C., R. A. Holman and M. F. Freilich (2003). "An optical technique for the measurement of longshore currents." *Journal of Geophysical Research* 108(C11): 3364.
- Diaz, M., M. Haller, B. Raubenheimer, S. Elgar and D. Honegger (2015). "Radar remote sensing estimates of waves and wave forcing at a tidal inlet." *Journal of Atmospheric and Oceanic Technology* 32(4): 842-854.
- Dongeren, A. v., N. G. Plant, A. Cohen, D. Roelvink, M. C. Haller and P. Catalan (2008). "Beach Wizard: nearshore bathymetry estimation through assimilation of model computations of remote observations." *Coastal Engineering* 55(12): 1016-1027.
- Flores, R. P., P. Catalan and M. Haller (2016). "Estimating surfzone wave transformation and wave setup from remote sensing data." *Coastal Engineering* 114: 244-252.
- Haller, M. and D. R. Lyzenga (2003). "Comparison of radar and video observations of shallow water breaking waves." *IEEE Transactions on Geosciences and Remote Sensing* 41: 832-844.
- Haller, M. C. and P. A. Catalan (2009). "Remote sensing of wave roller lengths in the laboratory." *Journal of Geophysical Research* 114.
- Haller, M. C., D. Honegger and P. Catalan (2014). "Rip current observations via marine radar." *Journal of Waterway, Port, Coastal and Ocean Engineering* 140: 115-124.
- Holman, R. A. and R. T. Guza (1984). "Measuring run-up on a natural beach." *Coastal Engineering* 8: 129-140.
- Holman, R. A. and M. C. Haller (2012). "Remote sensing of the nearshore." *Annual Reviews of Marine Science* 5: 95-113.
- Holman, R. A., N. G. Plant and K. T. Holland (2013). "cBathy: A robust algorithm for estimating

- nearshore bathymetry." *Journal of Geophysical Research* 118: 1-15.
- Honegger, D., M. C. Haller, W. R. Geyer and G. Farquharson (2017). "Oblique internal hydraulic jumps at a stratified estuary mouth." *Journal of Physical Oceanography*.
- Jessup, A. T., C. J. Zappa, M. Lowen and V. Hesany (1997). "Infrared remote sensing of breaking waves." *Nature* 385: 52-55.
- Konicki, K. and R. A. Holman (2000). "The statistics and kinematics of transverse sand bars on an open coast." *Marine Geology* 169: 69-101.
- Lippmann, T. C. and R. A. Holman (1989). "Quantification of sand bar morphology: A video technique based on wave dissipation." *Journal of Geophysical Research* 94(C1): 995-1011.
- Plant, N. G., K. T. Holland and M. Haller (2008). "Ocean wavenumber estimation from wave-resolving time series imagery." *IEEE Transactions on Geosciences and Remote Sensing* 46: 2644-2658.
- Ruessink, B. G., P. Bell, I. M. J. van Enckevort and S. G. J. Aarninkhof (2002). "Nearshore bar crest location quantified from time-averaged X-band radar images." *Coastal Engineering* 45: 19-32.
- Stockdon, H. F. and R. A. Holman (2000). "Estimation of wave phase speed and nearshore bathymetry from video imagery." *Journal of Geophysical Research* 105(C9): 22,015-022,033.
- Suanda, S. H., J. A. Barth, R. A. Holman and J. Stanley (2014). "Shore-based video observations of nonlinear internal waves across the inner shelf." *Journal of Atmospheric and Oceanic Technology* 31: 714-728.
- Wilson, G. W., H. T. Ozkan Haller, R. A. Holman, M. Haller, D. Honegger and C. C. Chickadel (2014). "Surf zone bathymetry and circulation via data assimilation of remote sensing observations." *Journal of Geophysical Research* 119(3).